Accuracy Assurance in Binary Interaction Approximation for N-Body Problems*)

Shun-ichi OIKAWA, Masaki GOTO, Kosuke HARUTA and Takanori KAMEI[1)]

Faculty of Engineering, Hokkaido University, N-13, W-8, Sapporo 060-8628, Japan

[1)]*Graduate School of Engineering, Hokkaido University, N-13, W-8, Sapporo 060-8628, Japan*

(Received 6 December 2011 / Accepted 1 June 2012)

Two accuracy assurance schemes are combined into the Binary Interaction Approximation (BIA) to N-body problems. The first one is a sort of variable time step (VTS) scheme for a given error tolerance. Since this scheme sometimes does not converge, an error-tolerance-adjusting (ETA) scheme is also introduced. With these two schemes combined into the original BIA, a significant improvement in terms of numerical error is obtained.

Keywords: binary interaction approximation, N-body problem, accuracy assurance, variable time step scheme, error tolerance adjustment, Runge-Kutta-Fehlberg

DOI: 10.1585/pfr.7.2401103

1. Introduction

We have proposed the Binary Interaction Approximation (BIA) scheme [1–3] to N-body problem. The BIA scheme views an N-body problem as the superposition of ${}_N\mathrm{C}_2$ two-body problems [1]. If we are interested in the motion of only one test particle-i at a time Δt from initial conditions at $t = 0$, it is possible with the BIA scheme to calculate $\boldsymbol{r}_i(\Delta t)$ and $\boldsymbol{v}_i(\Delta t)$ completely *in parallel*.

When the time interval Δt is chosen to be the time $\Delta\ell/g_{\mathrm{th}}$ for a particle with a mass m and its thermal speed of $g_{\mathrm{th}} = \sqrt{2T/m}$ to travel the average interparticle separation of $\Delta\ell = n^{-1/3}$ for plasmas with a temperature T and a number density n, the BIA is proven to be a powerful scheme for N-body problems [1]. Generally speaking, the BIA scheme is best suitable for fusion plasmas that are low-density and high-temperature gases. As will be shown later, however, for much longer time interval the BIA scheme may give erroneous results. In this study, we will introduce an accuracy-improving scheme to the BIA.

Equation of motion for the entire system is given as

$$m_i \frac{\mathrm{d}\boldsymbol{v}_i}{\mathrm{d}t} = \frac{Z_i e^2}{4\pi\varepsilon_0} \sum_{j\neq i}^{N} Z_j \frac{\boldsymbol{r}_i - \boldsymbol{r}_j}{\left|\boldsymbol{r}_i - \boldsymbol{r}_j\right|^3}. \tag{1}$$

It is practically impossible to deal with the large number of particles, i.e. $N \gg 1$, since the number of force calculations on the right-hand side of Eq. (1) is in proportion to N^2. Moreover, the number of time-steps tends to increase with increasing N, so the total CPU time should scale as $N^{2.3-3}$.

The efficient, fast algorithms to calculate interparticle forces include the tree method [4, 5], the fast multipole expansion method (FMM), and the particle-mesh Ewalt (PPPM) method [6]. Efforts have been made to use parallel computers and/or to develop special-purpose hardware to calculate interparticle forces, e.g., the GRAvity PipE (GRAPE) project [7].

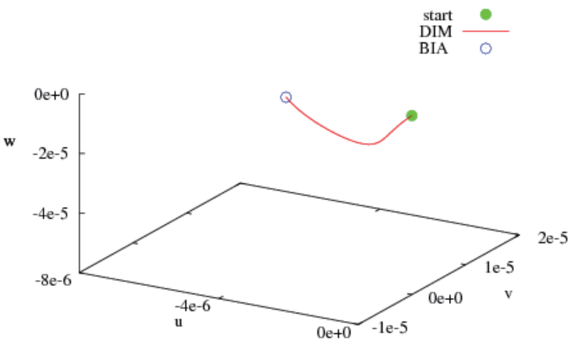

Fig. 1 A test calculation for a 1,332-body problem. A particle start at the point marked with a filled circle in green moves in the velocity space (u, v, w) along a red line, which is obtained by using a direct integration method (DIM), specifically a Runge-Kutta-Fehlberg scheme with an absolute error tolerance of 10^{-16}. The BIA gives the velocity at blue circle, which is close to the endpoint of the red line.

2. BIA Scheme

Let us now give a brief review on the BIA scheme. First choose a particle pair (i, j) from N particles as shown in Fig. 1. There are ${}_NC_2 = N(N+1)/2$ such combinations. The equation of motion for this case, instead of Eq. (1), is:

$$\mu_{ij} \frac{\mathrm{d}\boldsymbol{g}_{ij}}{\mathrm{d}t} = \frac{Z_i Z_j e^2}{4\pi\varepsilon_0} \frac{\boldsymbol{r}_{ij}}{r_{ij}^3}, \tag{2}$$

where $\boldsymbol{r}_{ij} = \boldsymbol{r}_i - \boldsymbol{r}_j$ is the relative position, $\boldsymbol{g}_{ij} = \boldsymbol{v}_i - \boldsymbol{v}_j$ is the relative velocity, and $\mu_{ij} = m_i m_i/(m_i + m_j)$ is the reduced

---

author's e-mail: masaki-g@fusion.qe.eng.hokudai.ac.jp

*) This article is based on the presentation at the 21st International Toki Conference (ITC21).

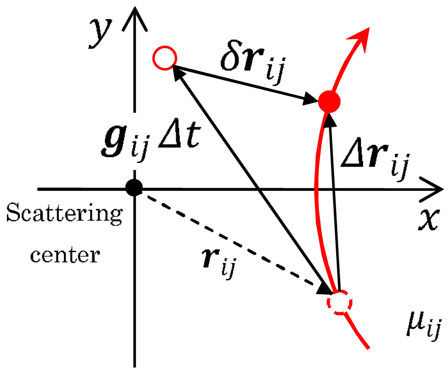

Fig. 2 Relative motion for a particle pair (i, j) in an orbital plane. Scattering center is at the origin. The change in position of the particle with a mass μ_{ij} is $\Delta\boldsymbol{r}_{ij}$. If no interaction occurs, the change in position is $\boldsymbol{g}_{ij}\Delta t$ during a time interval of Δt.

mass, $Z_i e$ is the electric charge of particle-i.

Since the exact solutions to two-body problems are known, for any time interval Δt the solution, $\boldsymbol{r}_{ij}(\Delta t)$ and $\boldsymbol{g}_{ij}(\Delta t)$ are easily found from the initial conditions $\boldsymbol{r}_{ij}(0)$ and $\boldsymbol{g}_{ij}(0)$. Once the solutions to all the two-body systems are found, changes in position and in velocity of individual particle during the time interval Δt is calculated as follows (see Appendix):

$$m_i\Delta\boldsymbol{r}_i = m_i\boldsymbol{v}_i\Delta t + \sum_{j\neq i}^{N}\mu_{ij}\left(\Delta\boldsymbol{r}_{ij} - \boldsymbol{g}_{ij}\Delta t\right), \tag{3}$$

$$m_i\Delta\boldsymbol{v}_i = \sum_{j\neq i}^{N}\mu_{ij}\Delta\boldsymbol{g}_{ij}. \tag{4}$$

Equation (4) for the velocity, i.e. momentum changes ensures the momentum conservation of the entire system. It should be noted that, unlike the changes in velocity $\Delta\boldsymbol{v}_i$, changes in position $\Delta\boldsymbol{r}_i$ due to particle j is not simple summation over $\Delta\boldsymbol{r}_{ij}$. As shown in Fig. 2, the subtraction by $\boldsymbol{g}_{ij}\Delta t$ from total change in position $\Delta\boldsymbol{r}_{ij}$ gives change in position due solely to the interaction between the pair (i, j). In the limit $\Delta t \to 0$, Eq. (3) reduces to the definition of velocity, and Eq. (4) reduces to the original equation of motion, as given in Eq. (1).

If we are interested in the motion of only one test particle-i at a time $t = \Delta t$ from the initial conditions at a time $t = 0$, it is possible with the BIA scheme to calculate $\boldsymbol{r}_i(\Delta t)$ and $\boldsymbol{v}_i(\Delta t)$ completely in parallel, since it is based on the principle of superposition of $\Delta\boldsymbol{r}_{ij}$ and $\Delta\boldsymbol{g}_{ij}$ using Eq. (3), and Eq. (4).

As shown in Fig. 1, the complicated change in velocity with time, or the acceleration, is typically reproduced well with the BIA (blue triangle) for a time interval of $1 \times \Delta t = \Delta\ell/g_{\rm th}$. For much longer time-interval of $100 \times \Delta t$, the red line in Fig. 3 represents the trajectory calculated by using a Runge-Kutta-Fehlberg integrator [8] with an absolute error tolerance of 10^{-16}. Note that the BIA scheme gives only the final solution at a given time interval, $100 \times \Delta t$ in this case, from the initial conditions. The final point due to the BIA calculation apparently deviates from that of the DIM. In the following section, we will introduce accuracy assurance schemes to the BIA to reduce the errors, or the deviation from the DIM.

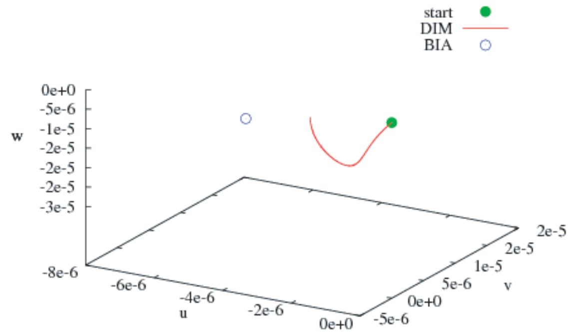

Fig. 3 A test calculation for a 1,332-body problem. Legends are the same as Fig. 1, except the final time is $100 \times \Delta t$. A particle start at the point marked with the filled circle in green moves in the velocity space (u, v, w) along a red line, which is obtained by using a direct integration method (DIM), specifically the Runge-Kutta-Fehlberg scheme. The BIA gives the velocity at blue circle, which is apparently not at the endpoint of the red line.

3. Accuracy Assured BIA Scheme

Suppose a general ordinary differential equation, for a time-dependent function $y = y(t)$, of the form:

$$\frac{dy}{dt} = f(y, t), \tag{5}$$

with an initial condition at a time $t = 0$ of

$$y(0) = y_0. \tag{6}$$

Let us define an exact time-shift operator $\mathcal{D}[y, \Delta t]$ on any time-dependent quantity:

$$\mathcal{D}\left[y(t), \Delta t\right] \equiv y\left(t + \Delta t\right). \tag{7}$$

Similarly let us introduce an operator:

$$\left.\begin{aligned} \mathcal{B}[\boldsymbol{r}_i, \Delta t] &= \boldsymbol{r}_i + \boldsymbol{v}_i\Delta t + \frac{1}{m_i}\sum_{j\neq i}^{N}\mu_{ij}\left(\Delta\boldsymbol{r}_{ij} - \boldsymbol{g}_{ij}\Delta t\right) \\ \mathcal{B}\left[\boldsymbol{v}_i, \Delta t\right] &= \boldsymbol{v}_i + \frac{1}{m_i}\sum_{j\neq i}^{N}\mu_{ij}\Delta\boldsymbol{g}_{ij} \end{aligned}\right\}, \tag{8}$$

which is an approximate operator to the exact operator $\mathcal{D}[y, t]$ with the BIA scheme described in the foregoing section, i.e. Eqs. (3)–(4).

3.1 Variable-time-step scheme

With these notations defined above, let $y_1(\Delta t)$ and $y_2(\Delta t)$ denote the approximate solutions at a time $t = \Delta t$,

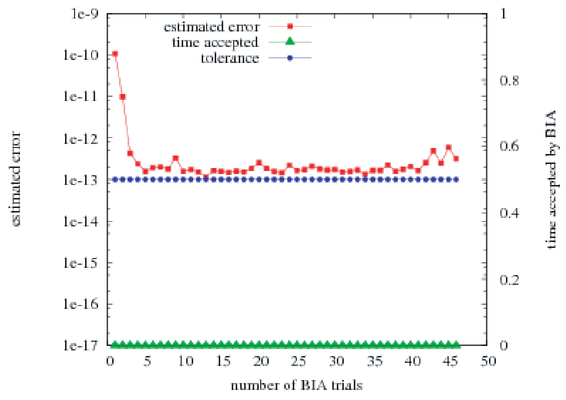

Fig. 4 Estimated errors vs. the number of BIA trials N_{trial} for $N = 1{,}332$. Since the error tolerance in blue, $\varepsilon = 10^{-13}$ is smaller than the estimated errors in red, the time step size becomes $\Delta/2^{N_{\mathrm{trial}}}$, where Δt is the initial one. Thus the time accepted by the BIA, plotted with green points, does not proceed.

as

$$y_1(\Delta t) = \mathcal{B}[y(0), \Delta t], \tag{9}$$

$$y_2(\Delta t) = \mathcal{B}[\mathcal{B}[y(0), \Delta t/2], \Delta t/2]. \tag{10}$$

Since the solution $y_2(\Delta t)$ is generally better than $y_1(\Delta t)$ in terms of numerical errors, we will choose an error tolerance ε_{T} in such a way that, if the following condition is satisfied,

$$|y_1 - y_2| < \varepsilon_{\mathrm{T}}, \tag{11}$$

we will accept the approximate solution $y_2(\Delta t)$. If not, the time interval is reduced, such as

$$\Delta t \rightarrow \Delta t/2, \tag{12}$$

then we will seek for an approximate solution $y(\Delta t/2)$ at $t = \Delta t/2$. Fortunately, $y_1(\Delta t/2)$ in the current stage

$$y_1(\Delta t/2) = \mathcal{B}[y(0), \Delta t/2], \tag{13}$$

has already been obtained in the first operation on $y(0)$, as shown in Eq. (10), in the previous stage. The procedure will be repeated until the time reaches the prescribed final time t_{end}.

For an N-body problem, the approximate position $\boldsymbol{r}_i$ and the velocity $\boldsymbol{v}_i$ at a time Δt, using the conventional BIA scheme, are formally represented as

$$\begin{aligned} \boldsymbol{r}_i(\Delta t) &= \mathcal{B}[\mathcal{B}[\boldsymbol{r}_i(0), \Delta t/2], \Delta t/2], \\ \boldsymbol{v}_i(\Delta t) &= \mathcal{B}[\mathcal{B}[\boldsymbol{v}_i(0), \Delta t/2], \Delta t/2]. \end{aligned} \tag{14}$$

It is sometimes the case that, as shown in Fig. 4, the estimated errors (in red) are never below the tolerance $\varepsilon_{\mathrm{T}} = 10^{-13}$ (in blue), so that the time (in green) does not proceed at all.

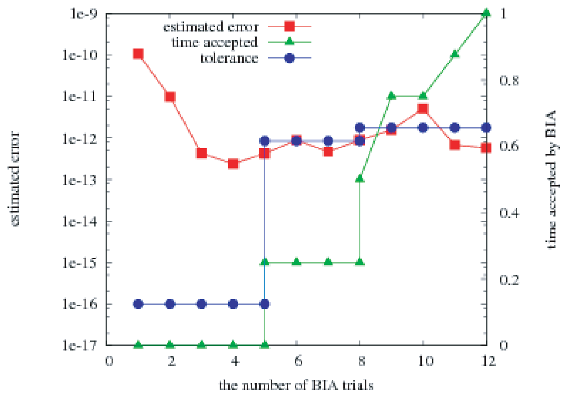

Fig. 5 Error-tolerance-adjusted BIA for the same case as in Fig. 4. The error tolerance adjustments occur at the 5th and 8th BIA trials. The vertical axis on the right is for the time accepted in green.

3.2 Error-tolerance-adjusting scheme

This problem was solved by the following tolerance adjusting scheme: It is usually the case that the estimated error rapidly decreases with decreasing time step size Δt for the first few BIA trials, irrespective of the errors being tolerable (accepted) or not. The dependence seems, by numerical investigation, to be

$$\varepsilon \propto \Delta t^{2-3}. \tag{15}$$

For the first few trials of the variable time step scheme explained above, estimated errors decrease rapidly. After such rapid decrement stage in estimated errors, the decrements become insensitive to the smaller time step Δt in some cases the estimated errors become larger for smaller time step size. Such an estimated error may be the attainable minimum error level by the BIA scheme. With this knowledge, the error tolerance is set twice the current one, when current estimated error is larger than one-fourth of the previous one, where one-fourth comes from the assumption that the estimated errors obey $\varepsilon \propto \Delta t^2$ for the rapid decreasing phase of the errors.

A test calculation with the error-tolerance-adjusting scheme is made for the same case presented in Fig. 3. Improvement against Fig. 4 is given in Fig. 5 and that for Fig. 3 in Fig. 6. In Fig. 4, the tolerance adjustments occur at the 5th and 8th BIA trials. In Fig. 6, the velocity at a time $100\Delta t$ given by the BIA with the error-tolerance-adjusting scheme is close to the by the DIM (Runge-Kutta-Fehlberg with an absolute error tolerance of 10^{-16}), as compared to that shown in Fig. 3. Thus the error-tolerance-adjusting scheme implemented into the BIA introduced in this study significantly improves the numerical accuracy of the BIA.

4. Summary

Two accuracy assurance schemes are introduced to the Binary Interaction Approximation (BIA) to N-body problems. The first one is a sort of variable time step

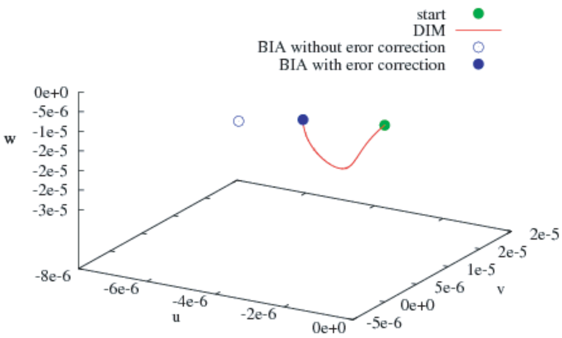

Fig. 6 A test calculation with the accuracy assured scheme for the same case as shown in Fig. 3. The filled circle in blue represents $v\,(100\Delta t)$ by using the BIA with the error correction scheme, while open circle in blue is that without as was shown in Fig. 3.

(VTS) scheme for a given error tolerance. Since this scheme sometimes does not converge, the error-tolerance-adjusting (ETA) scheme is also introduced. With these two schemes combined into the BIA, a significant improvement in terms of numerical error is obtained.

Acknowledgement

The authors thank Prof. Y. Matsumoto and Prof. M. Itagaki for fruitful discussions on the subject. This research was partially supported by a Grant-in-Aid for Scientific Research (C), 21560061.

Appendix A. Derivation of BIA Scheme

Since the force terms in Eq. (1) are the summation of those in Eq. (2), we have

$$\boldsymbol{f}_i = \sum_{j\neq i}^{N} \boldsymbol{f}_{ij}\left(\boldsymbol{r}_i, \boldsymbol{r}_j\right). \tag{A.1}$$

The exact change $m_i\Delta\boldsymbol{v}_i$ in momentum of the particle-i during a time-interval Δt is formally given as

$$\begin{aligned} m_i\Delta\boldsymbol{v}_i &= \int_t^{t+\Delta t} \boldsymbol{f}_i\left(\boldsymbol{r}_i(t), \boldsymbol{r}_j(t)\right) \mathrm{d}t \\ &= \sum_{j\neq i}^{N} \int_t^{t+\Delta t} \boldsymbol{f}_{ij}\left(\boldsymbol{r}_i(t), \boldsymbol{r}_j(t)\right) \mathrm{d}t. \end{aligned} \tag{A.2}$$

Since, in the framework of the BIA via Eq. (2), the relative force $\boldsymbol{f}_{ij}(t)$ changes the relative momentum $\mu_{ij}\boldsymbol{g}_{ij}(t)$,

$$\begin{aligned} m_i\Delta\boldsymbol{v}_i &\cong \sum_{j\neq i}^{N} \mu_{ij}\left[\boldsymbol{g}_{ij}(t+\Delta t) - \boldsymbol{g}_{ij}(t)\right] \\ &= \sum_{j\neq i}^{N} \mu_{ij}\Delta\boldsymbol{g}_{ij}, \end{aligned} \tag{A.3}$$

which is Eq. (4).

Similarly, the exact change $\Delta\boldsymbol{r}_i$ in position of the particle-i during Δt is formally given by

$$\begin{aligned} \Delta\boldsymbol{r}_i &= \int_t^{t+\Delta t} \boldsymbol{v}_i(t')\,\mathrm{d}t' \\ &= \int_t^{t+\Delta t} \left[\boldsymbol{v}_i(t) + \Delta\boldsymbol{v}_i(t')\right] \mathrm{d}t' \\ &= \boldsymbol{v}_i(t)\,\Delta t + \int_t^{t+\Delta t} \mathrm{d}t' \int_t^{t'} \frac{\mathrm{d}\boldsymbol{v}_i(t'')}{\mathrm{d}t''}\mathrm{d}t'', \end{aligned} \tag{A.4}$$

from which, with the BIA scheme, we have

$$\begin{aligned} m_i\Delta\boldsymbol{r}_i &\cong m_i\boldsymbol{v}_i(t)\,\Delta t + \int_t^{t+\Delta t} \mathrm{d}t' \int_t^{t'} \sum_{j\neq i}^{N} \mu_{ij} \frac{\mathrm{d}\boldsymbol{g}_{ij}(t'')}{\mathrm{d}t''}\mathrm{d}t'' \\ &= m_i\boldsymbol{v}_i(t)\,\Delta t + \int_t^{t+\Delta t} \mathrm{d}t' \sum_{j\neq i}^{N} \mu_{ij}\left[\boldsymbol{g}_{ij}(t') - \boldsymbol{g}_{ij}(t)\right] \\ &= m_i\boldsymbol{v}_i(t)\,\Delta t + \sum_{j\neq i}^{N} \mu_{ij}\left[\Delta\boldsymbol{r}_{ij} - \boldsymbol{g}_{ij}(t)\,\Delta t\right], \end{aligned}$$

which is Eq. (3).

[1] S. Oikawa and H. Funasaka, Plasma Fusion Res. **5**, S1051 (2010).
[2] S. Oikawa, K. Higashi and H. Funasaka, Plasma Fusion Res. **5**, S1048 (2010).
[3] S. Oikawa and H. Funasaka, Plasma Fusion Res. **3**, S1073 (2008).
[4] A.W. Appel, SIAM J. Sci. Stat. Comput. **6**, 85 (1985).
[5] J.E. Barnes and P. Hutt, Nature **324**, 446 (1986).
[6] P.P. Brieu, F.J. Summers and J.P. Ostriker, APJ **453**, 566 (1995).
[7] J. Makino, M. Taiji, T. Ebisuzaki and D. Sugimoto, APJ **480**, 432 (1997).
[8] E. Fehlberg, NASA Technical Report 315 (1969).